Separation Science and Technology
Publication details, including instructions for authors and subscription information:
http://www.informaworld.com/smpp/title~content=t713708471

Applicability of Activated Carbon to Treatment of Waste Containing Iodine-Labeled Compounds

H. M. H. Gad[a]; N. R. A. El-Mouhty[a]; H. F. Aly[a]
[a] Hot Laboratories and Waste Management Center, Egyptian Atomic Energy Authority, Cairo, Egypt

Online publication date: 22 June 2010

To cite this Article Gad, H. M. H. , El-Mouhty, N. R. A. and Aly, H. F.(2009) 'Applicability of Activated Carbon to Treatment of Waste Containing Iodine-Labeled Compounds', Separation Science and Technology, 44: 3, 681 — 711
To link to this Article: DOI: 10.1080/01496390802437172
URL: http://dx.doi.org/10.1080/01496390802437172

Separation Science and Technology, 44: 681–711, 2009

ISSN: 0149-6395 print/1520-5754 online
DOI: 10.1080/01496390802437172

Taylor & Francis
Taylor & Francis Group

Applicability of Activated Carbon to Treatment of Waste Containing Iodine-Labeled Compounds

H. M. H. Gad, N. R. A. El-Mouhty, and H. F. Aly
Hot Laboratories and Waste Management Center, Egyptian Atomic Energy Authority, Cairo, Egypt

Abstract: A timber industry waste was transformed to activated carbon by a one-step chemical activation process using H_3PO_4 (H). The used activated carbon (SDH) was characterized by N_2 adsorption, FTIR, density, pH, point of zero charge pH_{pzc}, moisture and ash content. Methylene blue (MB) and the iodine number were calculated by adsorption from the solution. The applicability of the different activated carbon produced was carried out to treatment of aqueous waste contaminated with iodine-labeled prolactin (I-PRL) Treatment processes were performed under the varying conditions; contact time, temperature, carbon type, carbon dosage, and different particle size of the activated carbon (SDH). The results indicated that 5 hours are sufficient to reach a plateau, and the amount of I-PRL adsorbed on SDH activated carbons increase with the solution temperature with thermodynamic parameter of $\Delta G^\circ = -7.962$ (kJ/mol), $\Delta H^\circ = 28.869$ (kJ/mol) and $\Delta S^\circ = 109.94$ (J/mol K). The optimum adsorption results were reached using carbon dose of 0.1 gm with particle size of <0.25 mm, and a batch factor (V/M) of 7.14 mlg^{-1}. First- and second-order equations, intra-particle diffusion equation, and the Elovich equation have been used to test experimental data. The experimental data was found to fit the second-order model and a chemisorptions mechanism. 0.7 M NaOH can be used for regeneration of spent SDH activated carbon with the efficiency of 99.6% and the regenerated carbon can be reused for five cycles effectively.

Keywords: Activated carbon, agricultural by-products, iodine-labeled prolactin, sawdust

Received 24 January 2008; accepted 10 July 2008.
Address correspondence to H. M. H. Gad, Department of Analytical Chemistry and Control, Hot Laboratories and Waste management Center, Egyptian Atomic Energy Authority, P.O. 13759 Cairo, Egypt. E-mail: hmhgad@yahoo.com

INTRODUCTION

Environmental pollution and its abatement have drawn keen attention for a long time. The problem of removing pollutants from water and wastewater has grown with rapid industrialization. Heavy metals, dyes, oil, and other salts, which are toxic to many living life and organisms, are present in the wastewater streams of many industrial processes, such as dyeing, printing, mining and metallurgical engineering, electroplating, nuclear power operations and/or isotopes production for radiotherapy, semiconductor, aerospace, battery manufacturing processes, etc. (1). All of these have faced increasing pressure regarding environmental and waste-related concerns as a result of the quantity and toxicity of generated wastewaters. Many methods have been used to remove the pollutants, namely, membrane filtration (2), coagulation (3), adsorption (4), oxidation (5), ion exchange (6), precipitation (7), etc. have been reported in the literature, but few of them were accepted due to cost, low efficiency, and inapplicability to a wide variety of pollutants.

The most widely used method for removing pollutants is coagulation and precipitation (7). A major problem with this type of treatment is the disposal of the precipitated waste. Another weak point is that in most cases the precipitation itself cannot reduce the contaminant far enough to meet current water-quality standards. Ion exchange treatment is the second most widely used method for metal removal. This method does not present a sludge disposal problem and has the advantage of reclamation of metals. It can reduce the metal ion concentration to a very low level. However, ion exchange does not appear to be practicable to wastewater treatment from a cost standpoint. Adsorption with activated carbon can also be highly efficient for the removal of numerous trace elements from water, but the high cost of activated carbon inhibits its large-scale use as an adsorbent. Therefore, the need for effective and economical removal of unwanted materials resulted in a research for unconventional methods and materials that might be useful in this field. The utilization of agricultural waste materials is increasingly becoming of vital concern because these unused resources are of little or no economic values, and some, such as sawdust, which are available in large quantities in lumber mills, often present a disposal problem. The use of sawdust for removing pollutants would benefit both the environment and wood agriculture in terms of decontamination of polluted water streams and to open a new market for the sawdust.

Radioimmunoassay (RIA) is a very sensitive technique to detect as low as quantity of hormone [prolactin (PRL), thyroglobulin (TG) etc.] in circulation or in any substance in biological fluids (8). Many essential reagents are required for RIA technique (9), the most important one

being the tracer. The tracers are the radioactive material that label the ligand of interest used in the RIA (10). Of all the isotopic labels used (I^{131}, P^{32}, I^{125}, S^{35}, H^3, C^{14}), the isotope I^{125} remains the ideal radioisotope of choice because of its sufficient long half-life (60.2 days), ease of iodination into tyrosyl residues of the biomlecules (11). Accordingly it represents the essential component of the waste produced from the RIA technique. Since the advent of radioactive waste management various approaches and technologies have been developed and adopted for the disposal and immobilization of radioactive aqueous wastes generated. The treatment process based on adsorption/ion exchange phenomenon plays an important role in pre-concentration/separation of toxic and hazardous radioactive materials from aqueous wastes (12,13). The sorption behavior of new adsorbents makes them promising candidates for application in radioactive aqueous waste treatment and are expected to play an important role in regulating the migration of radioactive materials.

In this study, the proposed research program is aimed at the investigation of the removal of organic compounds containing iodine using activated carbon prepared from a biomass material, sawdust (SD), by phosphoric acid (H_3PO_4) activation processes (SDH activated carbon). As the sorption characteristics of the adsorbents are controlled by a number of physico-chemical interfacial properties, it is of prime importance to evaluate their effects on the removal behavior of SDH towards wastewater containing organic compounds in the processes of production of labeled isotopes used as tracer in the radioimmunoassay.

EXPERIMENTAL

Preparation of Activated Carbon

Different agricultural by-products, e.g. rice husk (RH), sawdust (SD), apricot stone (AS), apricot stone core (ASC), apricot stone shell (ASS), bagasse pith (BP), olive stone (OS), and peach stone (PS) were chosen as precursors for the production of activated carbons by one-step chemical activation using H_3PO_4 (or KOH) to study the effect of the precursor nature on the adsorptive capacity of activated carbons. In each experiment, 30 g of the crushed precursor was soaked in 50 ml of pre-diluted phosphoric acid of 70 wt.% concentration starting with an 85 wt.% H_3PO_4 (BDH) (or 70% KOH, BDH) solution to cover it completely, slightly agitated to ensure penetration of the solution throughout. The mixture was heated to 80°C for 1 h and left overnight at room temperature to help appropriate wetting and impregnation of the precursor.

The impregnated mass was dried in an air oven at 80°C overnight, then, admitted into the reactor (ignition tube), which was then placed in a tubular electric furnace open from both ends. The temperature was raised at the rate of (50°C/10 min.) to the required end temperature. The carbonization process was carried out at 500°C for 80 min. The product was thoroughly washed with hot distilled water till pH = 6.5, and finally dried at 110°C. The prepared carbons and commercial activated carbon (Prolabo) were investigated in the preliminary test for removal of iodine labeled prolactin (I-PRL) and iodine labeled thyroglobulin (I-TG). The results are listed in Table 1.

Characterization of Activated Carbon

Packed and apparent densities were determined by a tamping procedure using a 10 ml graduated glass cylinder. Particle size was determined using sieves of different particle size. The texture characteristics were determined by the standard n_2 adsorption isotherms, followed by their analysis to evaluate the porous parameters. The total pore volumes estimated from the volume of nitrogen adsorbed at $p/p^\circ = 0.95$ (V_f) and an average pore radius from $r = 2V_p/S_{BET}$. The particle pore size distribution was

Table 1. Effect of activated carbon precursor on the removal of iodine-labeled compounds

No.	Types of precursors	% Removal	
		I-PRL	I-TG
1	*Rice husk (RHH)	92	82
2	Rice husk (RHK)	37	38
3	Sawdust (SDH)	96	81
4	Sawdust (SDK)	24	22
5	Bagasse pith (BPH)	93	60.8
6	Bagasse pith (BPK)	69.9	39.6
7	Apricot Stone (ASH)	94	33
8	Apricot Stone (ASK)	44.8	15
9	Olive stone (OSK)	28	19.5
10	Peach stone (PSK)	31	21
11	(AC + AS + RH; 1:1:1)H	92	44.3
12	(AC + AS + RH; 1:1:1)K	91	29.6
13	Commercial activated carbon	0.5	2

*Precursor followed by H, i.e., treated with H_3PO_4; and K, means that it treated with KOH.

determined in the Autosorb instrument (Quantachrome Inc.) using standard nitrogen adsorption at 77 K.

For iodine number determination (mg iodine/g carbon), 0.1 g of the sample was equilibrated for 1 h with a 0.1 N standardized iodine solution. The remaining iodine was titrated with a 0.1 N standardized sodium thiosulfate solution. The ash content of all samples was obtained after burning a given amount of carbon at 973 K for 3 h and was calculated on a dry basis (14). The pH of carbons was measured after suspending 1.0 g of the material in 20 ml CO_2-free distilled water for 48 h (14). The pH of zero point of charge (pH_{zpc}) of the SDH activated carbons was determined by adding a known amount of adsorbent to a series of 100 mL 0.01 N $NaNO_3$ bottles that contained various amounts of 0.01 N HNO_3 or 0.01 N NaOH. These bottles were rotated for 2 days in a shaker and the pH values were measured and recorded at the end of the test, then the solutions were adjusted to 0.1 M $NaNO_3$ by adding 2 mL of 5 M $NaNO_3$ into each bottle. These bottles were rotated for 2 more days in the shaker and the final pH was measured. The pH_{zpc} value for a specific adsorbent was at the pH value where the titration curves intercept. The surface charges of adsorbent can exhibit both positive and negative surfaces charges dependent on the solution pH. The pH corresponding to a surface charge of zero is defined as the zero point of charge (pH_{zpc}). Above the pH_{zpc} the surface charge will be negative and below the pH_{zpc} the surface charge will be positive. Therefore, an adsorbent with lower pH_{zpc} has higher cations adsorption capacities (30).

Methylene blue number was estimated by the extent of adsorption of milligrams of methylene blue adsorbed by 1 g of carbon in equilibrium with a solution of methylene blue having a concentration of 1.0 mg l^{-1}. Fourier transformed infrared spectroscopy (before and after adsorption of I-PRL) was used for the analyses of surface functional groups. The SDH activated carbon was analyzed for moisture content.

Preparation of Labeled Hormone

Iodogen is a mild oxidizing agent and it can be used for oxidation radioiodonation of proteins, polypeptides, hormones, and others. It is essentially insoluble in water. Therefore, it can be used as a thin film plated onto a bottom of glass vials.

Labeling Procedure: ^{125}I Labeling of PRL (or TG)

Ten micrograms of PRL (or TG) were incubated with 500 μCi/ml ^{125}I-Na and 10 μl 0.5 PO_4^{2-} (pH = 7.4) for 30 second at room temperature with

gentle shaking and 100 µl PO_4^{2-} (pH = 7.4) 0.05 M was then added to stop the reaction. Human prolactin (or thyroglobulin) was iodinated by the method of Hunter and Greenwood (8) and the iodinated hormone was separated from free iodine by gel filtration on a Sephadex column. The ^{125}I-PRL (or ^{125}I-TG) was eluted with 0.05 M PO_4^{3-} (pH = 7.4) and immediately placed on a Sephadex G-25 column to remove any damaged ^{125}I-PRL.

Kinetic Models Applied to the Sorption of I-PRL onto Sawdust Activated Carbon

In order to examine the controlling mechanism of the sorption process such as chemical reaction, diffusion control, and mass transfer, several kinetic models are used to test experimental data. From a system design viewpoint, a lumped analysis of the sorption rates is thus sufficient for practical operation (15).

1. First-order equation

The first-order equation is generally expressed as follows (16):

$$d_{qt}/dt = k_1(q_l - q_t) \tag{1}$$

After integration and applying the boundary conditions, for $q_t = 0$ at $t = 0$ and $q_t = q_t$ at $t = t$, the integrated form of Eq. (1) becomes:

$$\log(q_1 - q_t) = \log q_1 - (k_1/2.303)t \tag{2}$$

where q_1 and q_t (mg · g^{-1}) are the amounts of I-PRL sorbed at equilibrium and at time t (min.), respectively, and k_1 is the rate constant of first-order sorption (L · min^{-1}).

1. Second-order equation

If the rate of sorption is a second-order mechanism, the second-order chemisorption kinetic rate equation is expressed as (16):

$$dq_t/dt = k_2(q_2 - q_t)^2 \tag{3}$$

Integrating this equation for the boundary conditions, gives:

$$1/q_2 - q_t = 1/q_2 + k_2 t \tag{4}$$

which is the integrated law for a second-order reaction where q_2 is the amount of I-PRL sorbed at equilibrium ($mg \cdot g^{-1}$), k_2 is the equilibrium rate constant of second-order sorption ($g \cdot mg^{-1} \cdot min^{-1}$). Eq. (4) can be rearranged to obtain a linear form:

$$t/q_t = 1/k_2 q_2^2 + 1/q_2 t \tag{5}$$

and

$$h = k_2 q_2^2 \tag{6}$$

Where h is the initial sorption rate ($mg \cdot g^{-1}\ min^{-1}$).

1. Intraparticle diffusion equation

The fractional approach to equilibrium changes according to a function of $(Dt/r^2)^{1/2}$, where r is the particle radius and D the diffusivity of solute within the particle. The initial rate of the intraparticle diffusion is the following (17):

$$q_t = f(t^{1/2}) + I \tag{7}$$

The rate parameter (k_{int}) for intraparticle diffusion can be defined as:

$$q_t = k_{int} t^{1/2} + I \tag{8}$$

where k_{int} is the intraparticle diffusion rate constant ($mg \cdot g^{-1}\ min^{1/2}$) and I is the boundary layer ($mg \cdot g^{-1}$).

1. The Elovich equation

The Elovich equation is given as follows (18):

$$dq_t/d_t = \alpha e^{-\beta q t} \tag{9}$$

The integration of the rate equation with the same boundary conditions as the first- and second-order equations becomes the Elovich equation.

$$q_t = 1/\beta \ln(\alpha\beta) + 1/\beta \ln t \tag{10}$$

where α is the initial sorption rate ($mg \cdot g^{-1}\ min^{-1}$), and the parameter β is related to the extent of surface coverage and activation energy for chemisorptions (g/mg).

Distribution Coefficients (K_d)

The distribution coefficients (K_d) of I-PRL for SDH adsorbents was measured by batch adsorption experiments. The pH of experiments was adjusted to 7.0. In the batch adsorption experiment, the adsorbent was added to a known volume of the I-PRL solution, and was stirred at 298 K for interval times. The sample solution was separated from the adsorbent by centrifugation. The remaining activity of I-PRL was determined by gamma counter. The distribution coefficient was calculated as follows:

$$K_d = (A_i - A_e)/A_e \times V/W \tag{11}$$

where A_i is the initial activity of I-PRL in the solution, A_e is the equilibrium activity of I-PRL in the solution, V is the volume of the solution, W is the weight of the adsorbent (SDH). The percentage sorption was calculated from either of the following equations:

$$\% \text{ Sorption} = [(Ai - A)/Ai]100 \tag{12}$$

$$\% \text{ Sorption} = 100[K_d/(K_d + V/M)] \tag{13}$$

Regeneration Activated Carbon

After the attainment of equilibrium between the activated carbon and I-PRL, the supernatants were carefully decanted and desorption experiments for the loaded matrixes of SDH were carried out in aqueous medium of H_2O, HNO_3, and NaOH for regeneration of activated carbon and its reuse for several times.

RESULTS AND DISCUSSION

Effect of Particle Size

The experimental data for the adsorption of I-PRL onto SDH at different particle size of carbons (>1.0, >0.50, >0.25, <0.25 mm) at a fixed adsorbent dose are shown in (Fig. 1a). The results show that the I-PRL adsorbed is higher for a smaller adsorbent particle size. As the particle size increases from 0.25 to 1.0 mm, the uptake decreases from 70 to 63 $(\mu g \cdot g^{-1}) \times 10^{-3}$. This is because adsorption being a surface phenomenon, the smaller adsorbent particle sizes offered a comparatively large surface area and, hence, higher adsorption occurs at equilibrium. According to Weber Jr. (19), breaking of larger particles tends to open tiny cracks

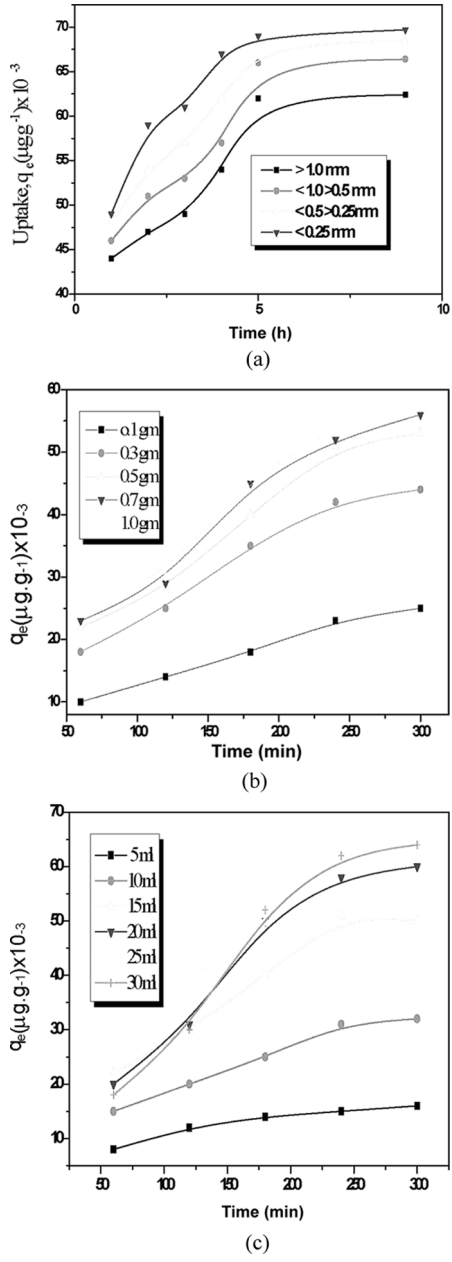

Figure 1. Effect of different factors on the adsorption of I-PRL onto SDH activated carbon; (a) Particle size, (b) Adsorbent dose, (c) Waste volume, and (d) Temperature.

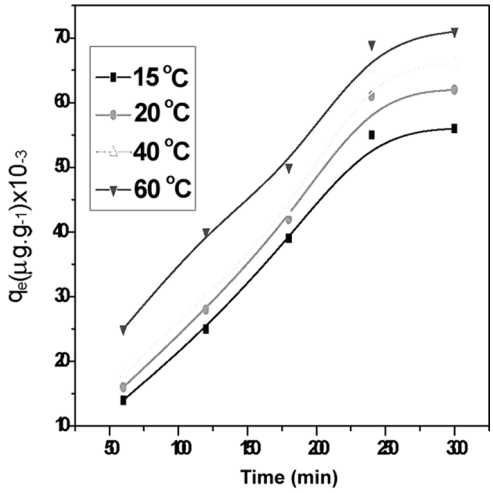

(d)

Figure 1. Continued.

and channels on the particle surface, providing an added surface area which can be employed in the adsorption process. The study also reveals that the size of the adsorbent particle is playing an important role in the adsorption process (20).

Numerous kinetic models have been proposed to elucidate the mechanism by which pollutants may be adsorbed. The mechanism of adsorption depends on the physical and/or chemical characteristics, the surface area of the adsorbent, as well as on the mass transport process. In order to investigate the mechanism of I-PRL adsorption, the four kinetic models previously mentioned are selected in this study (22). The applicability of the above four models can be examined by each linear plot of log $(q_1 - q_t)$ versus t, (t/q) versus t, q_t versus ln t and q versus $t^{0.5}$, respectively and are presented in (Fig 2). In order to quantify the applicability of each model for a different particle size of activated carbon, the correlation coefficient (r^2) was calculated from these plots and listed in Table 2. The linearity of these plots indicates the applicability of the four models. However, the analyses of the correlation coefficients (r^2) showed that the experimental data ($r^2 > 0.98$) fit the second-order model (an indication of a chemisorptions mechanism) better than the first-order model (r^2 ranging between 0.839 and 0.978). The rate of adsorption (k), and initial sorption rate (h) were decreased with an increase in the SDH activated carbon particle size as shown from Table 2.

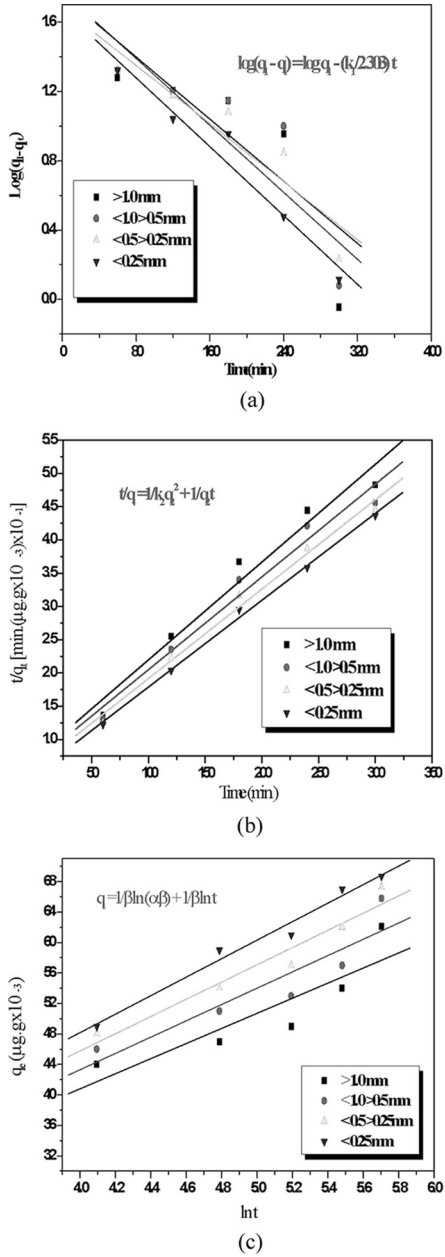

Figure 2. Kinetic parameters of four kinetic model of sorption of I-PRL onto SDH activated carbon at different particle size; (a) First order reaction, (b) Second order reaction, (c) Elovich equation, and (d) Intraparticle diffusion.

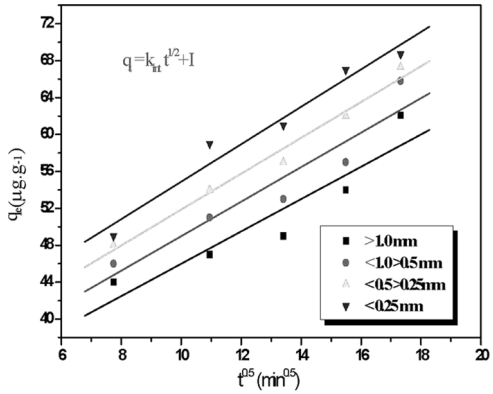

(d)

Figure 2. Continued.

The values of the maximum adsorption capacity determined using the linear transformation of the Elovich equation Table 2 are much lower than the experimental adsorbed amounts at equilibrium corresponding to the plateau of the adsorption process, in spite of the good correlation coefficients. This means that the assumption of the exponential covering of adsorption sites is not in agreement with the experiment in the studied concentration range (21).

The intraparticle diffusion was also involved in the adsorption of I-PRL by SDH activated carbons. The linear portion of the plot for a wide range of contact time between the adsorbent and the adsorbate does not pass through the origin. This deviation from the origin or near saturation may be due to the difference in the rate of mass transfer in the initial and final stages of adsorption (22). Further, such deviation from origin indicates that the pore diffusion is not the only rate controlling step. From Fig. 2, it may be seen that, there are two regions, the initial pore diffusion due to external mass transfer followed by the intraparticle diffusion. Generally, (as shown from Table 2) as the particle size decreases, the adsorption capacity and the rate of adsorption increase with best correlation coefficient at the particle size of <0.25 mm with the four kinetic models.

The values of intercept, I, in the intraparticle diffusion equation Table 2 give an idea about the boundary layer thickness, i.e. the larger the intercept, the greater is the boundary layer effect. The boundary layer diffusion depends on several parameters, including the external surface area of the adsorbent, which is mainly controlled by the particle size (as the particle size decreases, the boundary layer increases in our

Table 2. Kinetic parameters for the effects of SDH particle size and dose on sorption of I-PRL

		First-order kinetic equation log $(q_1-q_t)=\log q_1-(k_1/2.303)\,t$			Second-order kinetic equation $t/q_t=1/k_2q_2^2+1/q_2t$				The Elovich equation $q_t=1/\beta\ln(\alpha\beta)+1/\beta\ln t$			Intraparticle diffusion equation $q_t=k_{int}t^{1/2}+I$		
Parameters	q_e, exp ($\mu g\cdot g^{-1}$) $\times 10^{-3}$	q_1 ($\mu g\cdot g^{-1}$) $\times 10^{-3}$	$k_1(1\cdot min^{-1})$ $\times 10^{-3}$	r^2	$q_2(\mu g\cdot g^{-1})$ $\times 10^{-3}$	$k_2(g\cdot(\mu g\ min)^{-1})$ $\times 10^{-4}$	h ($\mu g\cdot g^{-1}\cdot min^{-1})^{-7}$ $h=k_2q_2^2$	r^2	α (Initial sorption rate)	β (surface coverage)	r^2	k_{int} ($\mu g\cdot(g\ min^{0.5})^{-1}$)	r^2 int	I ($\mu g\cdot g^{-1}$)
>1.0 mm	63	59.87	11.1	0.839	67.98	2.982	13.780	0.982	3.32	0.100	0.887	1.752	0.931	28.74
>0.5 mm	67	57.21	10.3	0.849	71.68	2.975	15.285	0.985	1.66	0.093	0.915	1.869	0.948	30.29
>0.25 mm	69	48.41	9.65	0.928	74.40	3.155	17.464	0.994	1.72	0.088	0.971	1.942	0.990	32.43
<0.25 mm	70	47.43	11.5	0.978	76.56	3.591	21.048	0.998	0.68	0.082	0.989	2.029	0.980	34.95
0.1 gm	25	35.16	14.82	0.947	43.27	1.019	1.907	0.969	4.053	0.104	0.977	1.634	0.993	3.226
0.3 gm	44	80.09	14.07	0.953	76.10	0.618	3.623	0.976	3.019	0.058	0.982	2.919	0.989	5.108
0.5 gm	54	109.9	14.87	0.919	95.41	0.441	4.014	0.937	2.856	0.048	0.964	3.564	0.980	7.484
0.7 gm	56	85.70	12.04	0.967	92.33	0.562	4.791	0.991	2.812	0.046	0.968	3.747	0.980	7.658
1.0 gm	58	87.29	11.97	0.959	100.2	0.455	4.568	0.960	2.731	0.045	0.962	3.775	0.977	6.424
5 ml	16	16.0	11.56	1.000	21.05	5.0472	2.236	0.999	4.574	0.202	0.996	0.821	0.979	2.336
10 ml	32	58.89	15.06	0.923	48.03	1.3912	3.209	0.983	3.252	0.089	0.981	1.898	0.989	3.059
15 ml	50	88.54	14.35	0.948	82.71	0.6611	3.523	0.967	2.806	0.052	0.971	3.264	0.977	3.789
20 ml	60	152.3	16.77	0.961	140.6	0.1915	3.786	0.947	2.835	0.037	0.979	4.559	0.979	15.41
25 ml	65	141.42	15.82	0.930	148.5	0.2371	5.229	0.988	2.673	0.039	0.991	4.379	0.991	8.265
30 ml	64	189.66	17.41	0.953	232.6	0.0596	4.225	0.964	2.854	0.032	0.977	5.276	0.979	23.31
15°C	56	174.4	16.76	0.911	352.1	0.0193	2.393	0.631	1.107	0.035	0.973	4.807	0.983	26.62
20°C	62	212.1	17.68	0.895	328.9	0.0252	2.726	0.693	1.074	0.032	0.969	4.472	0.981	26.51
40°C	66	243.4	18.42	0.878	283.2	0.0376	3.015	0.722	1.056	0.031	0.961	5.493	0.977	24.94
60°C	71	181.1	16.32	0.898	145.3	0.2253	4.757	0.954	0.982	0.033	0.976	5.501	0.986	15.24

investigation), the shape and density of the particles, the concentration of the solution and the agitation velocity. The greater the particle size, the greater the intraparticle diffusion resistance (23), and this was confirmed by lower rate of adsorption as seen in Table 2.

Effect of SDH Activated Carbon Dose

The results of the effect of SDH activated carbon dose are shown in Fig. 1b. Kinetic parameters from linear plots (Fig. 3) of the four kinetic models are given in Table 2. The data for I-PRL again show a good compliance with the second-order equation and the regression coefficients, r^2, for the linear plots were all higher than those of the first-order equation confirming again that the adsorption is chemisorptions mechanism. From the data listed in Table 2, it is clear that:

i. For first and second-order equation; the rate of adsorption increases as the adsorbent dose decreases with the best result for 0.1 gm of SDH activated carbon. But, the best correlation coefficient was obtained with 0.7 gm i.e. at a batch ratio $(V/M) = 7.1$.

ii. The initial rate of adsorption of a second-order reaction increases with the increase of carbon dose and this is may be due to the larger surface area available at high carbon dose.

iii. From the Elovich equation, the initial sorption rate and surface coverage have a conversely relationship with carbon dose with the highest values with 0.1 gm carbon dose.

iv. The linear plots of q_t versus $t^{0.5}$ at a different carbon dose show that the rate of adsorption (k_{int}) has a direct relationship with the carbon dose confirming that the increase in carbon dose leading to higher surface area available for adsorption of I-PRL. On the other hand, the boundary layer increases with an increase of carbon dose and carbon dose of 0.1 gm has lowest boundary layer with the best correlation coefficient (0.993).

Waste Volume Effect

The experimental results of the sorption of I-PRL on SDH at different waste volume are shown in Fig. 1c. The sorption capacities at equilibrium, q_e, increase from 16×10^{-3} to $65 \times 10^{-3}\,\mu g \cdot g^{-1}$ with an increase in the waste volume from 5 to 30 ml with a 1.5 gm dose of SDH.

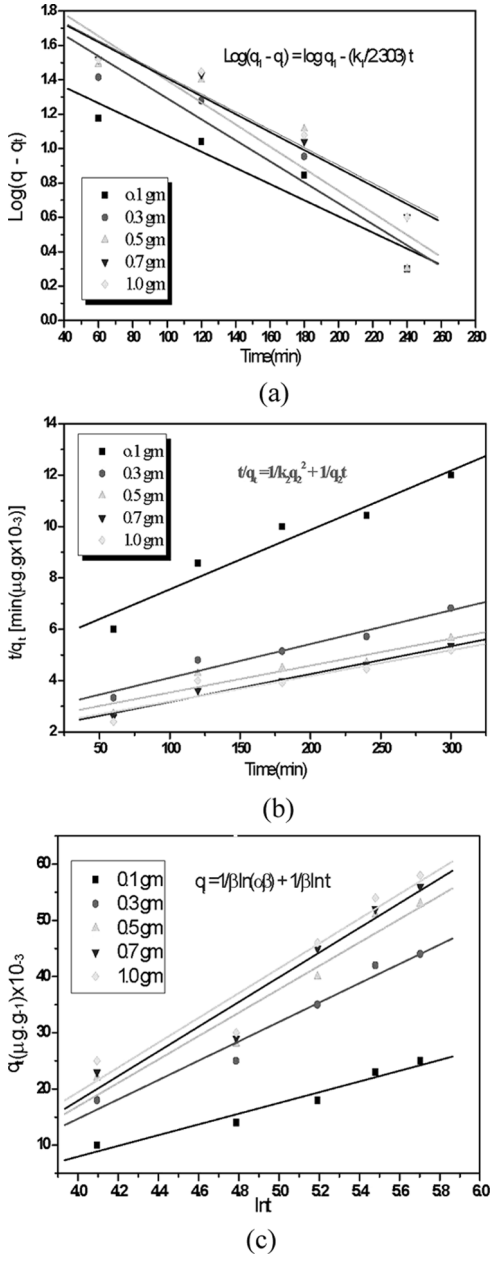

Figure 3. Kinetic parameters of four kinetic model of sorption of I-PRL onto SDH activated carbon at different carbon dose; (a) First order reaction, (b) Second order reaction, (c) Elovich equation, and (d) Intraparticle diffusion.

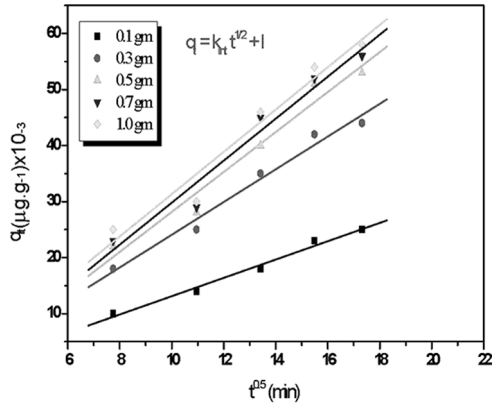

(d)

Figure 3. Continued.

Figure 4 shows the parameters of the four kinetic model of sorption of I-PRL onto SDH activated carbon at different waste volume. The characteristic parameters of all the kinetic models and correlation coefficients are tabulated in Table 2. Again, correlation coefficients of second-order equation are higher than those of first-order equation. This suggest that the sorption systems studied belong to the second-order kinetic model, based on the assumption that the rate limiting step may be chemical sorption or chemisorptions involving valence forces through sharing or exchange of electrons between sorbent and sorbate. Similar phenomena have also been observed in biosorption of dyes RB2, RY2, and Remazol Black B on the biomass (24). For the second-order model:

a. The rate constant decreases with an increasing of waste volume, this is logic due to the increase of resistance for I-PRL molecule to reach the surface of the adsorbent with the increase of waste volume, and this is confirmed by:

   1. Increasing the boundary layer in the intraparticle diffusion.
   2. Decreasing the surface coverage, β, in the Elovich equation.

b. The initial sorption rate, h, increases with an increasing of waste volume (due to increase of concentration of I-PRL with higher waste volume), and this is also confirmed by:

   1. significant increase in the adsorption capacities (q_2).
   2. Increasing the rate of intraparticle diffusion, K_{int}, with increasing waste volume.

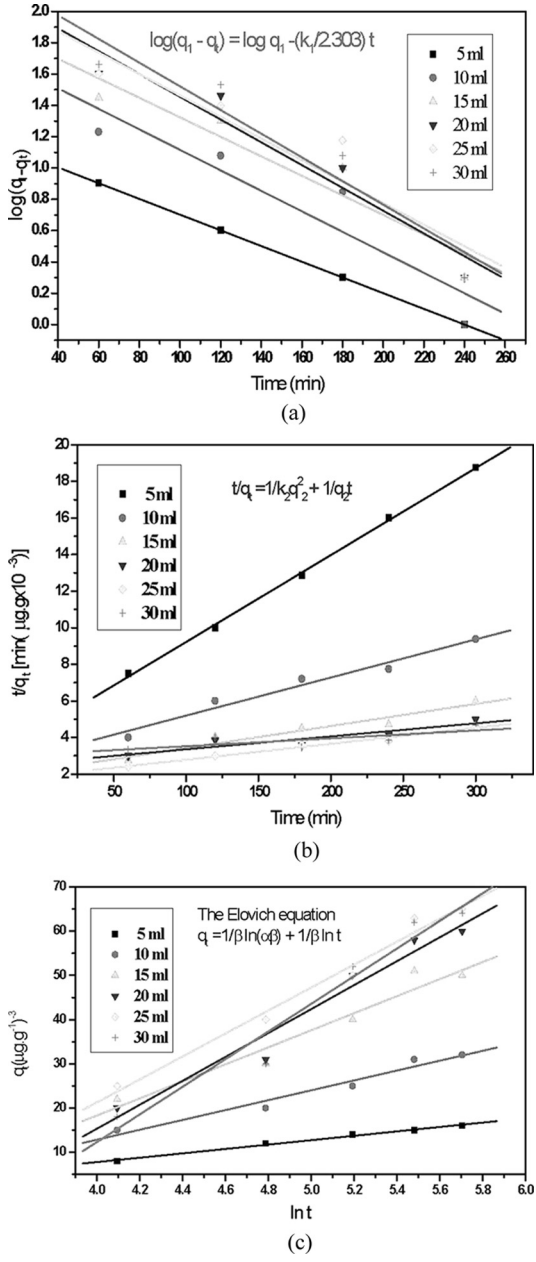

Figure 4. Kinetic parameters of four kinetic model of sorption of I-PRL onto SDH activated carbon at different waste volume; (a) First order reaction, (b) Second order reaction, (c) Elovich equation, and (d) Intraparticle diffusion.

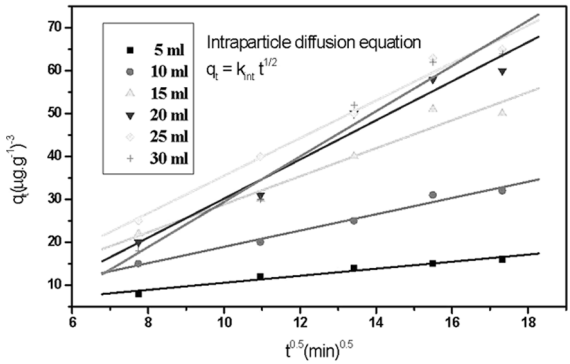

(d)

Figure 4. Continued.

The agreement of the Elovich equation with experimental data may be explained as below. The previous successful applications of the Elovich equation to heterogeneous catalyst surfaces helps to explain its success in predicting the sorption of I-PRL on SDH activated carbon. The general explanation for this form of kinetic law involves a variation of the energetic of chemisorptions with the active sites are heterogeneous sawdust and therefore, exhibit different activation energies for chemisorptions (15). Because the cell walls of sawdust mainly consist of cellulose and lignin, and many hydroxyl groups, such as tannins or other phenolic compounds (15,31).

Effect of Temperature

Temperature has a direct influence on the amount of the adsorbed substance. In the present investigation, the adsorption experiments were performed in the temperature range of 15–60°C. It was found that, (Fig. 1d), that the amount of I-PRL adsorbed on SDH activated carbons increase with the solution temperature. Figure 5 shows the parameters of the four kinetic model of sorption of I-PRL onto SDH activated carbon at different temperature, and the results are given in the Table 2. It is observed that the correlation coefficients of the intraparticle diffusion equation are higher than those of the other three kinetic models. The results also show that k_{int} is an increasing function of the solution temperature. The increase of k_{int} with temperature indicates that the affinity for I-PRL is favored by high temperature, and therefore, this adsorption

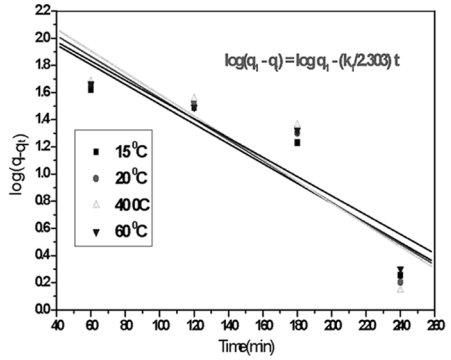

(a)

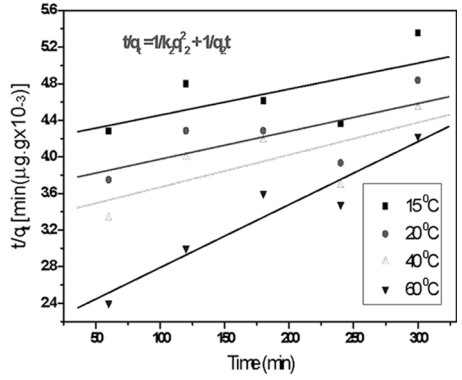

(b)

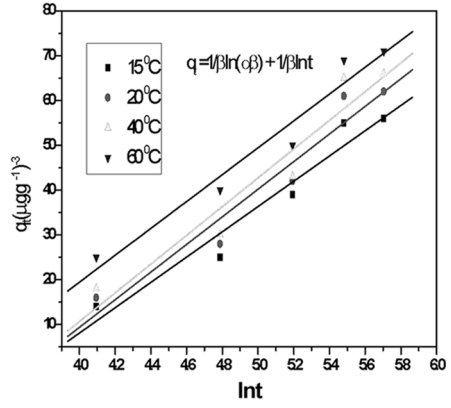

(c)

Figure 5. Kinetic parameters of four kinetic model of sorption of I-PRL onto SDH activated carbon at different temperature; (a) First order reaction, (b) Second order reaction, (c) Elovich equation, and (d) Intraparticle diffusion.

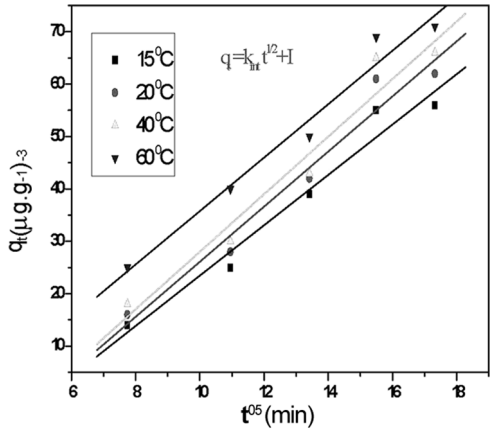

Figure 5. Continued.

process is endothermic in nature. The increase in capacity, q_e, with respect to temperature indicates that:

a. some kind of chemical interaction may take place during adsorption process.
b. Our sample has high porosity (microporous), k_{int} values increases with increase of temperature that is why mobility of I-PRL molecules increases.

However, I (boundary layer thickness) values decrease with increase k_{int} values and temperature. The results of the present investigation on the effect of temperature also support the conclusion that I-PRL sorption is controlled by pore diffusion.

Thermodynamic Parameters of Adsorption

Effect of temperature on the I-PRL adsorption is shown in Fig. 1d. As the temperature increases, the adsorption capacities of I-PRL removal increases, indicating the adsorption to be endothermic. The change in standard free energy (ΔG°), enthalpy (ΔH°) and entropy (ΔS°) of adsorption were calculated from the following equation (25):

$$\Delta G^\circ = -RT \ln K_c \tag{14}$$

where R is the gas constant (8.314 J/mol K), K_c is the equilibrium constant and T is temperature in K.

The *K*c value is calculated from Eq. (15):

$$K_c = C_{Ae}/C_{Se} \tag{15}$$

where, C_{Ae} and C_{Se} are the equilibrium concentration of I-PRL on adsorbent ($mg \cdot L^{-1}$) and in the solution ($mg \cdot L^{-1}$), respectively. Van't Hoff plots of I-PRL adsorption onto SDH for different temperatures is given in Fig. 6.

Standard enthalpy (ΔH°) and entropy (ΔS°), of adsorption can be estimated from Van't Hoff equation given in:

$$\ln Kc = -\Delta H^\circ_{ads}/RT + \Delta S^\circ/R \tag{16}$$

The slope and intercept of the Van't Hoff plot is equal to $-\Delta H^\circ_{ads}/R$ and $\Delta S^\circ/R$, respectively. Thermodynamic parameters obtained are summarized in Table 3. The endothermic nature of process is well explained by positive value of the enthalpy change. The negative value of free energy suggests that the adsorption process is spontaneous and the affinity of the adsorbent for the I-PRL is indicated by the positive value of entropy (25).

Effect of Agitation Time

Removal of I-PRL by SDH activated carbons with time was carried out at pH = 7 and a temperature of 20°C (Fig. 7a). The amount of I-PRL

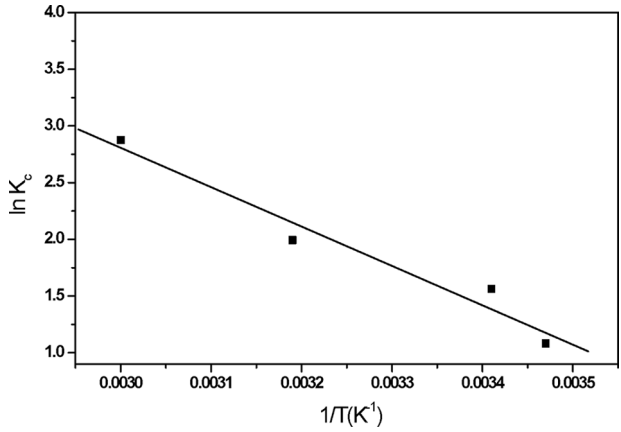

Figure 6. Van't Hoff plots of I-PRL adsorption onto SDH activated carbon for different temperatures.

Table 3. Thermodynamic parameters for the adsorption of I-PRL onto SDH activated carbon

Temperature (K)	K_c	$-\Delta G^\circ$ (kJ/mol)	ΔH°(kJ/mol)	ΔS°(J/mol K)
288	2.947	2.588	28.869	109.94
293	4.769	3.805		
313	7.333	5.183		
333	17.75	7.962		

adsorbed increases with agitation time and attain equilibrium at about 180 min for SDH activated carbons. Therefore, an optimum agitation period of 5 h was selected. The curves shown in Fig. 7a present a double

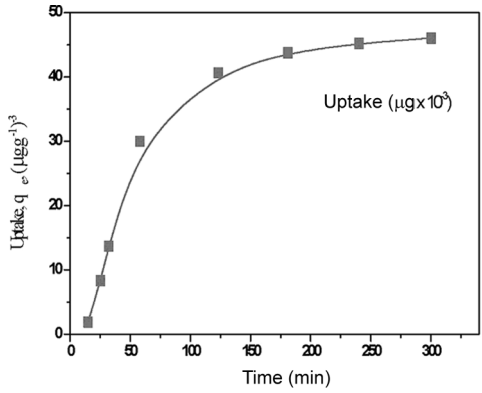

(a)

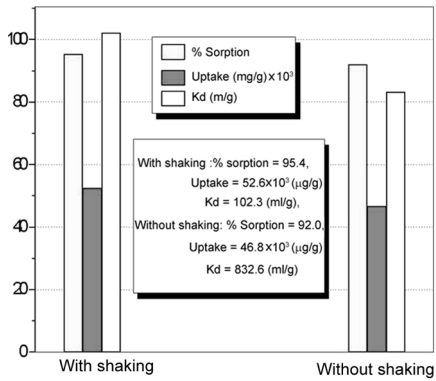

(b)

Figure 7. Effect of agitation time (a) and shaking process (b) on I-PRL removal by SDH activated carbons.

nature, the initial portion of the curve rises linearly and is changed into a curve and levels off after 5 h of contact time. The plateau portion of the curve corresponds to pore diffusion and the linear portion of the curve reflects surface layer diffusion (20).

Only contact between the waste solution of I-PRL and the SDH adsorbent for 5 h (without shaking) leads to sorption percent of 92.1, this sorption percent increase to 95.3 with shaking of 300 rpm. This may indicate that the shaking process increases the chance of the inter particle diffusion of I-PRL and the adsorbate interpenetrates through the adsorbent easily with subsequent increase of the % sorption as shown in the (Fig. 7b).

Distribution Coefficient (K_d)

The distribution coefficient K_d, which defines the affinity of the I-PRL for the SDH adsorbent was determined and listed in Table 4. The K_d is commonly used as a means of assessing the mobility of radionuclides in the environment and for comparing adsorption data obtained from different sources. While the K_d values in laboratory batch experiments should not be assumed to be identical to field sorption values, this type of partitioning information can be used to compare the likely mobility of radionuclides in the environment (26).

From the results shown in Table 4 it is clear that:

1. As the particle size decreases, the K_d increases and this is may be due to the increase of surface area of the adsorbent with the small particle size at fixed batch ratio (V/M).
2. The K_d decreases with the increase of the mass of adsorbent. This is may be due to the increase of resistance of inter particle diffusion with the decrease in batch ratio as shown from the Table 4.
3. On the contrast to mass of adsorbent, as the waste volume increases, (i.e. increase of the concentration) the K_d increases due to the lower resistance at higher batch ratio.
4. As expected, the increasing of temperature leads to increasing the K_d and this may be due to the increase the mobility of adsorbate molecules toward the adsorbent surface at fixed batch ratio.

Adsorption interaction in this case must involve some type of specific interaction at higher temperature, i.e., probable bond cleavage (endoprocess) to result in smaller entities feasible to certain pore size. Alternatively, such behavior may be ascribed to "activated" adsorption which accelerates diffusion into certain pores in the adsorbent (27).

Table 4. The distribution coefficient of the adsorption of I-PRL onto SDH activated carbon at different experimental conditions

	Particle size (mm)				Adsorbent dose (gm)					Waste volume (ml)						Temperature (°C)			
Values	>1.0	>0.50	>0.25	<0.25	0.1	0.3	0.5	0.7	1.0	5	10	15	20	25	30	15	20	40	60
K_d	36.02	56.36	75.93	91.07	24.76	23.29	22.13	20.4	16.58	0.89	4.9	19.62	51.64	103.25	111.42	20.52	32.82	49.66	112.96
V/M	7.14	7.14	7.14	7.14	50	16.66	10	7.14	5	3.33	6.6	10	13.33	16.66	20	7.14	7.14	7.14	7.14

K_d = Distribution coefficient (ml/g). V = Volume of the sample (ml). M = Mass of adsorbent (gm).

Table 5. Factors affecting on desorption and regeneration of I-PRL from loaded SDH activated carbon

	Desorbing agents (0.5 Mol.)			NaOH concentration (Mol.)					Volume of NaOH (ml)						Number of cycle				
	H_2O	HNO_3	NaOH	0.1	0.3	0.5	0.7	0.9	1	2	3	4	5	10	1	2	3	4	5
%	0.42	5.3	65	24	40	65	99.6	97.6	19	30	50	65	96	97	99.6	91	87	84	80
V/M	10	10	10	10	10	10	10	10	2	4	6	8	10	20	10	10.2	10.4	11.1	11.9

Desorption and Regeneration

Desorption of the adsorbed I-PRL from the spent adsorbent SDH was also studied. It was found that there are four parameters significantly affect of desorption and regeneration process:

a. *Type of desorbing agent*: The carbon loaded with the maximum amount of I-PRL were placed into desorption medium containing H_2O, 0.5 M HNO_3 and 0.5 M NaOH and the amount of I-PRL desorbed in 4 h was measured and the result are listed in Table 5. The 0.5 M of NaOH give the higher value of desorption percent.
b. *Effect concentration of NaOH*: 0.7 M of NaOH is the best concentration as shown from Table 5. This may be due to the higher concentration of OH^- ions which replace I-PRL leading to high desorption percent.
c. *Effect of batch ratio (V/M)*: as the batch ratio increases, desorption percent increases which is related to the ease by which the OH^- can be replace the I-PRL molecules.
d. *Number of regeneration cycle*: the SDH activated carbon can be used for 5 cycles effectively.

From Table 5 the desorption percent decreased from 99.6 to 80% after 5 cycle, which is most probably related to the loss of sorbant weight (approximately 14% loss).

Characterization of SDH Activated Carbon

Figure 8a demonstrates nitrogen adsorption isotherms of SDH carbon. It is clear that this isotherm show mixture of Type I and Type II in BDDT classification (28). A pore size distribution of SDH activated carbons is displayed in Fig. 8b. It can be seen that SDH carbons does not contain macropores. Phosphoric acid activated SDH carbon exhibit two large peaks; one in micropore range and the other in mesopore range. The main adsorption characteristics of the carbon are summarized in Table 6. It is clear that SDH activated carbon has different porous structure. The total surface area of SDH is $1254\,m^2 \cdot g^{-1}$, of which 52% is contained in micropores. Thus, the amount of mesopores is 48%. The total pore volume of SDH is $0.923\,cm^3/g$, of which 44.64% is contained in micropores and the amount of mesopores is 55.36%.

The FTIR analysis showed that various oxygen containing groups of acidic character (hydroxyl and carbonyl groups) with different chemical properties are present on the carbon surface. The spectrum of the

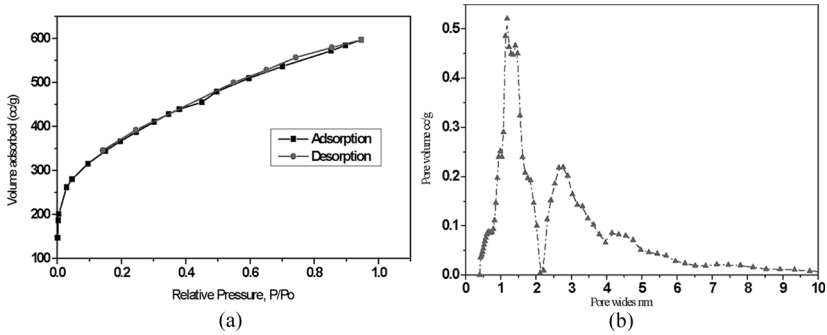

Figure 8. Adsorption isotherms of N2 at 77 K (8a) and pore size distribution (8b) for SDH activated carbons.

sawdust pre-impregnated with 70% H_3PO_4 solution displayed the following bands: 3419.2 cm^{-1} due to bonded O–H, at 2926.2 cm^{-1} to C–H vibrations. The band at 1636.8 cm^{-1} for carbonyl groups (C = O). The band at 1159.1 cm^{-1}: assigned to C–O–C strong symmetrical band, at 1009.2 cm^{-1} assigned to out of plane bending C–H bond (29).

These functional groups contributed to larger amounts of I-PRL adsorbed onto the SDH activated carbons. However, these functional

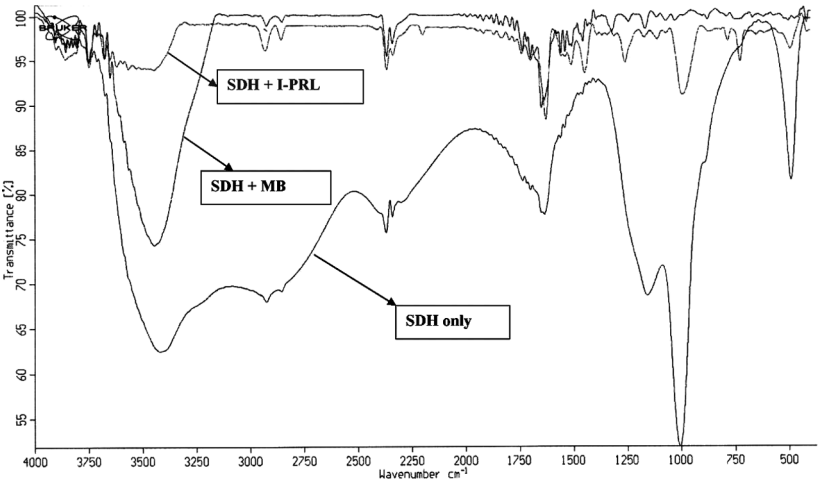

Figure 9. Show the contribution of surface functional groups of SDH activated carbon in the removal of both MB and I-PRL. (SDH only = FTIR of activated carbon, SDH + MB = FTIR of activated carbon after adsorption of Methylene Blue, SDH + i – PRL = FTIR of activated carbon after adsorption of I-PRL.)

Table 6. Physicochemical characterization of SDH activated carbon

No.	Control tests	SDH activated carbon	No.	Control tests	SDH activated carbon
1	Carbon yield (%)	75	11	Micrpore surface area ($m^2 \cdot g^{-1}$)	652
2	Ash content (%)	8.5	12	Iodine number ($mg \cdot g^{-1}$)	1340
3	Moisture content (%)	7	13	Methylene blue number ($mg \cdot g^{-1}$)	340
4	Packed density ($g \cdot ml^{-1}$)	1.18	14	Phenol number (mg)	50
5	Apparent density($g \cdot ml^{-1}$)	0.812	15	Matter soluble in water (%)	1.9
6	BET surface area ($m^2 \cdot g^{-1}$)	1254	16	Matter soluble in acid (%)	2.32
7	Total pore volume ($cm^3 \cdot g^{-1}$)	0.923	17	Matter soluble in base (%)	2.21
8	Micropore volume ($cm^3 \cdot g^{-1}$)	0.412	18	pH	3.6
9	Mesopores volume ($cm^3 \cdot g^{-1}$)	0.511	19	Point of zero charge (pH_{pzc})	3.8
10	Average pore radius (nm)	1.5	20	Particle size (mm)	Range of >.0 to <0.25

groups disappeared or have very low intensity after the adsorption process, which confirm that these groups contribute in the removal of I-PRL, confirming that the process of I-PRL removal using SDH in this study is dependant on both the surface area and the surface functional groups.

Economic Study

The relative cost of the materials used in the present study is very much lower than commercial activated carbons. The sawdust is available almost free of cost and after considering the expenses for transport, chemicals, and electrical energy the cost of the final adsorbent materials would be approximately less than 1/6 the cost of the cheapest variety of carbons used for water treatment. Due to the high heating value of sawdust village people may use it for making fire briquettes. This is an alternative method of disposal of sawdust activated carbon.

CONCLUSION

The results of this work can be summarized as follows:

1. New alternative adsorbents for treatment of waste containing I-PRL have been explored by making chemical activations of some agricultural-byproducts by phosphoric acid. This study showed that activated carbon prepared from sawdust is the best one for the removal of I-PRL and this may be due to a high surface area ($1254\,m^2 \cdot g^{-1}$) and the presence of many surface functional groups (FTIR).
2. The kinetics of sorption of I-PRL onto SDH was studied by using first-order and second-order equations, intraparticle diffusion, and the Elovich equation. The sorption kinetics of I-PRL was studied as a function of particle size, mass of adsorbent, waste volume, and the temperature of the system. For all the systems examined, the second-order kinetic model provided the best correlation of the experimental data. The second-order equation is based on the sorption capacity on the solid-phase and is in agreement with a chemisorption mechanism being the rate controlling step.
3. The sorption of I-PRL onto SDH can also be successfully interpreted by the Elovich equation. This supports the heterogeneous nature of SDH adsorbent surface likely to be responsible for I-PRL uptake.
4. The uptake of I-PRL was found to be controlled by external mass transfer at earlier stages and by intraparticle diffusion at later stages. The adsorption of I-PRL was found to be endothermic indicating that the adsorption (and distribution coefficient, K_d) would be enhanced at temperature above the ambient temperature, and the agitation slightly increases the uptake than the static sorption process. The SDH activated carbon can be regenerated and recycled five times effectively with 0.7 M NaOH and the economic cost was estimated.

NOTE

From Author to the Editor: This manuscript has not been published elsewhere and it has not been submitted simultaneously for publication elsewhere.

REFERENCES

1. Alka Shukla; Yu-Hui Zhang; Dubey, P.; Margrave, J.L.; Shyam Shukla, S. (2002) The role of sawdust in the removal of unwanted materials from water. *Journal of Hazardous Materials*, *95* (1–2): 137.

2. Brandon, C.A.; Johnson, J.S.; Mintura, R.E.; Proter, J.J. (1973) *Text Chem. Color*, *5*: 134.
3. Ibrahim, N.A.; Hashem, A.; Abou-Shosha, M.H. (1997) Animation of wood sawdust for removing anionic dyes from aqueous solutions. *Polymer-Plastics Technology and Engineering*, *36* (6): 963.
4. Faustt, S.D.; Osman, A.M. (1987) *Adsorption Processes for Water Treatment*; Butterworth: Stockholm, MA.
5. Kabita, Dutta; Sekhar, Bhattacharjee; Basab, Chaudhuri; Subrata, Mukhopadhyay. (2002) Chemical oxidation of C. I. Reactive Red 2 using Fenton-like reactions. *J. Environ. Monit.*, *4*: 754.
6. Sarzanini, C.; Mentaasti, E.; Porta, V. (1988) In: *Ion Exchange for Industry*, Streat, M., ed.; Ellis Horword: Chichester, UK, 189.
7. Cushnie, G.C. (1984) *Removal of Metals from WasteWater: Neutralization and Precipitation*; Noyes Publications: Park Ridge, NJ.
8. Greenwood, F.C.; Hunter, W.M.; Glover, J.S. (1963) *Biochem. J.*, *89*: 114.
9. Borth, R.; Lumenfield, B.; Dewatte, V.H. (1957) *Acta. Endocrinol.*, *24*: 119.
10. Bristow, A.F.; Georing, A.T.H.; Thrope, R. (1990) In: *Radioisotopes in Biology, A Practical Approach Stated*, R. G. Oxford University Press, 242.
11. Hamilton, R.S. (1987) In: *Immunoassay a Practical Guide*, Chon, D.W.; Perlstein, M.T., eds.; Academic Press, Inc.: USA, 35, 38.
12. Carley-Macanly, K.W. (1984) Option for the treatment of low- and intermediate-level active liquid wastes. In: *Proc. Int. Conf. Radioactive Waste Management*, IAEA: Vienna, 2: 15.
13. Levi, H.W. (1963) Fixation of radionuclides in TiO2 and titanates via coprecipitation. In: *Treatment and Storage of High Level Radioactive Wastes Proc. Symp.*; IAEA: Vienna, 587.
14. Polymnia, Galiatsatou; Michail, Metaxas; Vasilia, Kasselouri-Rigopoulou. (2002) Adsorption of zinc by activated carbons prepared from solvent extracted olive pulp. *Journal of Hazardous Materials*, *91* (1–3): 187.
15. Mahmut, Özacar; Ayhan, I.; Engil, S. (2005) A kinetic study of metal complex dye sorption onto pine sawdust. *Process Biochemistry*, *40* (2): 565.
16. Ho, Y.S.; McKay, G. (1999) Pseudo-second order model for sorption processes. *Process Biochemistry*, *34* (5): 451.
17. Özacar, M. (2003) Equilibrium and kinetic modeling of adsorption of phosphorus on calcined alunite. *Adsorption*, *9*: 125.
18. Cheung, C.W.; Porter, J.F.; McKay, G. (2000) Sorption kinetics for the removal of copper and zinc from effluents using bone char. *Sep Purif Technol*, *19*: 55.
19. Weber, W.J. Jr. (1967) In: *Principles and Applications of Water Chemistry*, Faust, S.A.; Hunter, J.V. eds.; Wiley: New York.
20. Anoop Krishnan, K.; Anirudhan, T.S. (2002) Removal of mercury (II) from aqueous solutions and chlor-alkali industry effluent by steam activated and sulphurised activated carbons prepared from bagasse pith: kinetics and equilibrium studies. *Journal of Hazardous Materials*, *B92*: 161.

21. Oualid, Hamdaoui. (2006) Batch study of liquid-phase adsorption of methylene blue using cedar sawdust and crushed brick. *Journal of Hazardous Materials*, *B135*: 264.
22. Kaustubha, Mohanty; Das, D.; Biswas, M.N. (2005) Adsorption of phenol from aqueous solutions using activated carbons prepared from *Tectona grandis* sawdust by $ZnCl_2$ activation. *Chemical Engineering Journal*, *115*: 121.
23. Onal, Y.; Akmil-Basar, C.; Didem Eren, C.; Igdem Sarici, Ozdemir; Tolga, epic. (2006) Adsorption kinetics of malachite green onto activated carbon prepared from Tunc bilek lignite. *Journal of Hazardous Materials*, *B128*: 150.
24. Aksu, Z.; Tezer, S. (2000) Equilbrium and kinetic modelling of biosorption of Remazol Black B by Rhizopus arrhizus in a batch system: Effect of temperature. *Process Biochem*, *36*: 431.
25. Önal, Akmil-Başar C.; Sarici-Özdemir, Ç. (2007) Investigation kinetics mechanisms of adsorption malachite green onto activated carbon. *Journal of Hazardous Materials*, *146* (1–2): 194.
26. Sheppard, M.I.; Thibault, D.H. (1990) Default soil solid/liquid partition coefficients K_{ds}, for four major soil types: a compendium. *Health Physics*, *59*: 471.
27. Daifullah, A.A.M.; Girgis, B.S.; Gad, H.M.H. (2004) A study of the factors affecting the removal of humic acid by activated carbon prepared from biomass materials. *Colloids and Surfaces A: Physicochem. Eng. Aspects*, *235*: 1.
28. Brunauer, S.; Deming, L.S.; Deming, W.S.; Teller, E. (1940) On a theory of the van der Waals adsorption of gases. *J. Amer. Chem. Soc.*, *62*: 1723.
29. Moreno-Castilla, C.; Lopez-Ramon, M.V.; Carrasco-Marin, F. (2000) Changes in surface chemistry of activated carbons by wet oxidation, *Carbon*, *38*: 1995.
30. Fan, H.J.; Anderson, P.R. (2005) Copper and cadmium removal by Mn oxide-coated granular activated carbon. *Separation and Purification Technology*, *45* (1): 61–67.
31. Mishra, S.P.; Tiwari, D.; Prasad, S.K.; Dubey, R.S.; Mishra, M. (2007) Biosorptive behavior of mango (*Mangifera indica*) and neem (*Azadirachta indica*) bark samples for 134Cs from aqueous solutions: A radiotracer study. *J. Radioanal. Nucl. Chem.*, *272*: 371–379.